Anisotropy of optical properties of hexagonal boron nitride films

L. V. Kotova[a], *, L.A. Altynbaev[a], M. O. Zhukova[b], B.T. Hogan[c, d], A. Baldycheva[c], D. M. Kurbatov[a], and V. P. Kochereshko[a]

[a] Ioffe Institute, St. Petersburg, 194021 Russia
[b] St. Petersburg National Research University of Information Technologies, Mechanics, and Optics (ITMO University), St. Petersburg, 197101 Russia
[c] Department of Engineering, University of Exeter, Exeter EX4 4QF, United Kingdom
[d] OPEM, ITEE, University of Oulu, 90014 Oulu, Finland
e-mail: kotova@mail.ioffe.ru

Abstract. Thin hexagonal boron nitride films with a thickness of several monoatomic layers have been manufactured by splitting of bulk samples in an ultrasonic bath. The transmission, reflection, and photoluminescence spectra of such films are studied. The spectral dependences of linear and circular polarization of light passing through the sample are measured. Scanning electron microscopy investigation demonstrates homogeneity of the obtained samples. However, investigation of Stokes parameters of light passing through the sample makes it possible to reveal hidden anisotropy of optical properties of these films.

Keywords: boron nitride, optical anisotropy, spectroscopy, polarization, thin films

1. Introduction

In recent years, two-dimensional atomically thin materials attract special interest of researchers. In particular, these systems are associated with opportunities of creating van der Waals heterostructures in which two-dimensional layers of different semiconductors are arranged one after another. Such structures, owing to the strong covalent bond inside layers and relatively weak bond between layers, preserve many properties of the initial materials. When creating heterostructures, owing to the weak van der Waals bond between layers, there is no need to take care of lattice matching, which allows one to use the full range of two-dimensional materials without regard to the magnitude of the lattice parameter.

The most prominent representative of two-dimensional semiconductors is graphene, a monolayer of carbon atoms located at nodes of the two-dimensional hexagonal lattice. Graphene is a semimetal with a zero bandgap. The bandgap of other compounds varies from zero to 6 eV, which makes it possible to obtain heterostructures with a very wide range of properties.

The interest in thin layers of hexagonal boron nitride is caused by stability of the compound in the two-dimensional form and graphene-like structure. For this reason, boron nitride is one of most suitable materials for heterostructure barrier layers, with great opportunities for being used in nanoelectronics [1] and optoelectronics [2].

The simplest and most wide-spread technology for obtaining thin, up to monoatomic layers of such materials is mechanical cleavage of layers with an adhesive tape. However, this method of manufacturing nanostructures can be hardly called progressive. Different methods are developed to refine the technology of manufacturing thin layers of graphene-like materials. One of promising technologies is cleavage of thin layers of layered semiconductors by use of ultrasound in a bath with a fluid. However, this technology is also not free from disadvantages because it yields films with a random size and location distribution of microcrystals.

In this work, manufacturing of thin hexagonal boron nitride films by ultrasonic cleavage of bulk boron nitride and the experimental investigation of their optical properties are described. In particular, photoluminescence spectra upon photoexcitation by lasers with different wavelengths, transmission and reflection spectra, and spectral dependences of Stokes parameters of light passing through the sample with linear and circular polarization at normal incidence are studied.

2. Experimental

Thin hexagonal boron nitride (h-BN) films were obtained on a polyethylene terephthalate substrate by the following method. Bulk h-BN powder was initially dispersed in a mixture of isopropanol and deionized water

at the ratio of 60:40. After energetic shaking for maximum disaggregation and dispersion of h-BN particles, the solution was then subjected to ultrasonic treatment in an ultrasonic bath (James Products 120 W High Power 2790ml Ultrasonic Cleaner) filled with deionized water. To provide sufficient cleavage of the sample, five periods with a duration of 30 min each were used to prevent excessive heating of the solvent. Then, the obtained dispersions were centrifuged during 10 min at 2000 rpm to crash the remaining bulk material and to narrow the size distribution of particles which are present in the dispersion. After centrifuging, the dispersion was divided into fractions; in this process, only the nondeposited fraction was extracted to ensure the presence of only appropriately sized particles. Then, the obtained dispersion was dried in vacuum (at a pressure of ~0.1 atm) on a Schlenk line for complete removal of the solvent. The obtained powder with a mass of 606 mg was then dispersed again in 12 mL of isopropanol mixed with 8 mL of deionized water with the obtained concentration of about 30 mg/mL. This redispersed solution was treated by ultrasound during additional 30 min to provide homogeneous dispersion.

To obtain homogeneous thin films of multilayered h-BN layers laid on each other, the redispersed solution was filtered through a microporous (with a pore size of 0.2 μm) polytetrafluoroethylene membrane. Such films were widely studied for different two-dimensional materials and it was shown that dispersions of graphene oxides and molybdenum disulfide yielded high-quality films [3–7]. The thin films obtained as a result of dispersion filtration were transported or deposited by the method described above [8–10]. The widespread use of this technology points to simplicity and scalability of the method of extended integration of the two-dimensional material. The membrane was transferred to the desired substrate; in this process, the filtered 2D-material contacted with the substrate. The membrane was moistened by isopropanol. Then, the substrate was heated to 70°C, isopropanol was vaporized, and h-BN was released from the membrane. This process is compatible with many different substrates. The thin ~1 cm2 films obtained in this way were successfully transferred to the substrate for further measurements.

The images of the surface of the obtained samples are presented at different magnification in Figs. 1a–1c. These images demonstrate that this sample is a conglomerated powder consisting of thin crystalline BN plates with the transverse size from 5 μm and less and with a thickness from ten monoatomic layers to one. Visually, these microcrystals are oriented completely chaotically. The sample surface has no preferred directions both on the scale of hundreds of microns and on the scale of several microns.

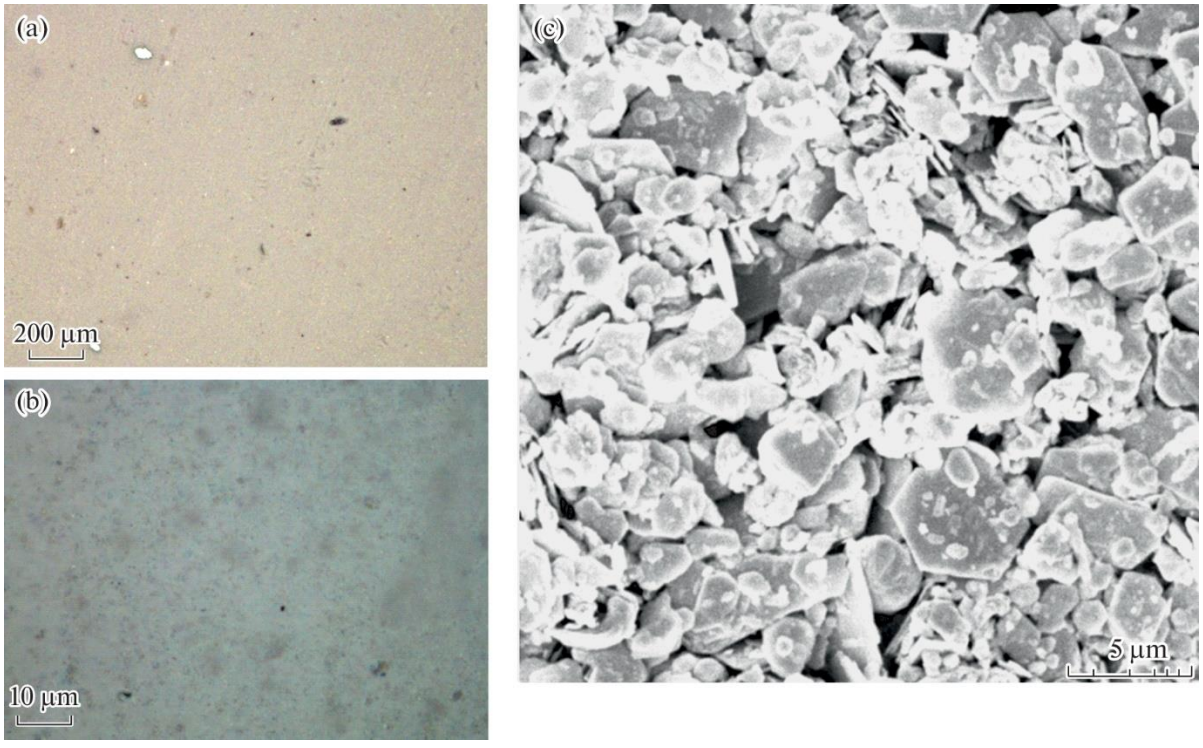

Fig. 1. Images of the sample surface at different magnification obtained using (a, b) an optical microscope in nonmonochromatic light and (c) a scanning electron microscope.

We studied photoluminescence, reflection, and transmission spectra of polarized light of these samples at room temperature. The spectra were obtained on a facility consisting of a CCD-equipped spectrometer with a focal length of 0.5 m. Photoluminescence was excited using lasers with radiation wavelengths $\lambda = 244$ (5.08 eV), 532 (2.33 eV), and 662 nm (1.87 eV). The transmission and reflection spectra were registered using a halogen lamp.

To corroborate the crystalline structure of the sample, the Raman scattering spectrum was taken. The spectrum demonstrated the presence of a crystalline structure corresponding to the structure of hexagonal boron nitride crystals. At the same time, a rather intense diffuse background indicating a large number of defects was observed.

A wide photoluminescence (PL) band with a width of about 1 eV and a maximum at energy of 3.6 eV was observed in PL spectra upon excitation with a wavelength of 224 nm above the indirect bandgap edge. Upon excitation by radiation with energy below the fundamental absorption edge of an ideal h-BN crystal, a set of narrow lines in the energy region of ~1.5 eV was also observed.

The presence of radiation bands in the bandgap depth points to the fact that they can be related to deep-level impurities and to color centers. The dependence of the photoluminescence spectrum on the exciting light energy points to the fact that intracenter transitions are also observed along with zone–vacancy transitions. Calculations show that the position of photoluminescence maximums of thin films correlates with energies of transitions to energy levels of color centers [11, 12].

As seen in Figs. 1a and 1b, the sample surface is matte. At the same time, mirror reflection from the surface is almost absent and strong Rayleigh light scattering is observed.

We have measured Rayleigh scattering spectra as functions of the angle of light incidence on the sample (angle Φ in Fig. 2) in the angle interval from zero to 45° and of the azimuthal angle between the plane of incidence and the sample edge (angle Θ in Fig. 2) in the interval from 0° to 360°. The spectra had no structure but one wide maximum with a width of 1 eV at energy of 1.7 eV. It was found that the scattered light intensity did not depend on the azimuthal angle Θ. With a change in the angle of incidence Φ, no qualitative differences between the spectra were revealed but a change in their general intensity.

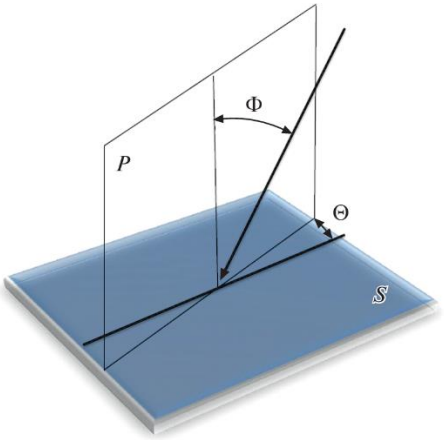

Fig. 2. Scheme of the experiment: P is the plane of incidence, S is the sample surface, Φ is the angle of incidence, and Θ is the azimuthal angle between the plane of incidence and the sample edge.

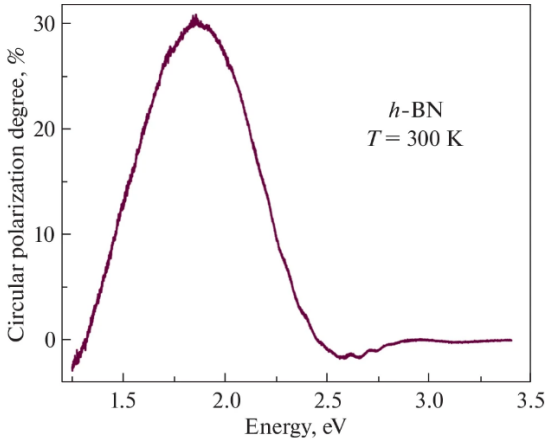

Fig. 3. Spectral dependence of the circular polarization degree of the h-BN sample transmission.

In the transmission spectra, strong absorption was observed in the region inside the h-BN bandgap as early as at energies above 3 eV, with a feebly marked structure. In the region of transparency from 1.3 to 3.0 eV, no interference features were observed in transmission spectra, which suggests that the sample thickness noticeably changes on scales on the order of the light beam size (~1 mm).

We performed measurements of transmission spectra of polarized light in the region of transparency of the sample and measured Stokes parameters of light passing through the sample. The measured quantities were the circular polarization degree (Fig. 3), the linear polarization degree (Fig. 4a), and the linear polarization degree in axes turned around 45° (Fig. 4b).

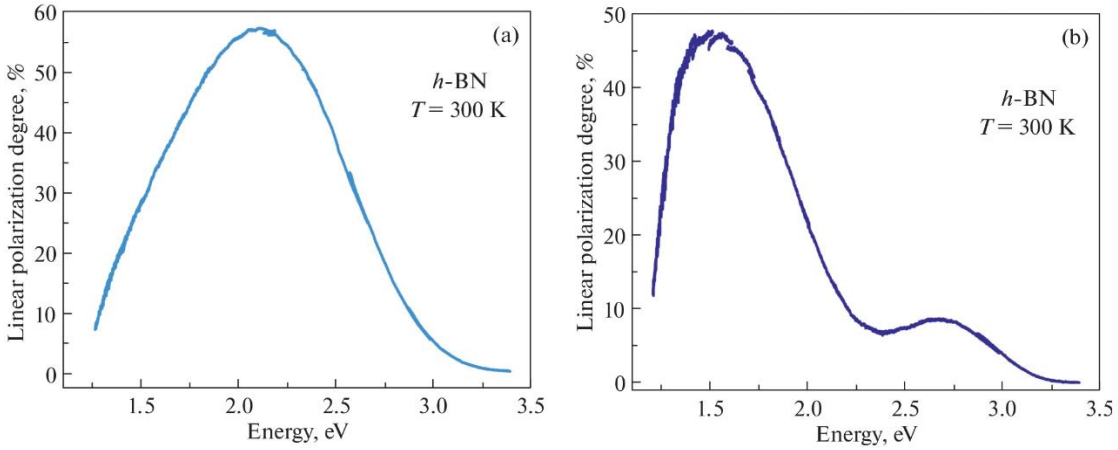

Fig. 4. Spectral dependence of the linear polarization degree of h-BN transmission: (a) in the (x, y) axes, polarization of the incident light is directed along the x axis; (b) in the (x', y') axes turned around 45° relative to the (x, y) axes; the z axis is directed along the normal to the sample surface.

The obtained data unambiguously imply that the phenomenon of light birefringence is observed in the whole measured spectral interval. This phenomenon manifests itself in conversion of linear polarization to elliptical. At a wavelength of 550 nm, the circular polarization changed its sign. This is the isotropic point in the spectrum at which the birefringence sign changes. At the same time, this effect reaches the maximum at a wavelength $\lambda \sim 650$ nm.

The spectral dependences of the linear polarization degree corroborate the conclusion about the presence of birefringence and allow one to determine the direction of optical axes.

The phenomenon of birefringence was measured depending on the point at the sample. It turned out that the direction of the optical axis did not change over the whole sample area ($\sim$1 cm^2).

3. Discussion

It is evident that the birefringence is caused by the presence of a preferred optical axis in the sample under study. The appearance of an optical axis in the powder can be caused both by anisotropy of powder particles themselves and by anisotropy of their position [13]. However, anisotropy of only powder particles themselves cannot lead to anisotropy of the whole sample but, certainly, can lead to local anisotropy.

Individual hexagonal crystals of boron nitride are really anisotropic. The indices of light refraction along the hexagonal axis and perpendicularly to it are very much different [14]. In the BN powder, orientation of crystals, as seen from Fig. 1c, is quite chaotic (at least on scales from 200 to 1 μm). Therefore, the birefringence cannot be caused by anisotropy of BN microcrystals themselves.

However, polarization measurements unambiguously point to the presence of such anisotropy. Moreover, it has been found that the direction of the optical axis is the same over the whole sample area. This suggests that the cause of anisotropy is not hidden in properties of individual crystals but is common for the whole sample and manifests itself over long (centimeter) distances. It has been verified that the substrate itself is optically isotropic. Changes in light reflected/scattered from the sample demonstrate that, in contrast to the case described in [15], the slope of microcrystals in the powder is also chaotic.

The presence of hidden order in unordered powder can suggest that we deal with a finite system of microcrystals in which there is no complete averaging of properties. A similar case in which naked-eye scattering was absent but anisotropic light scattering took place was modeled theoretically in [13].

To describe the observed phenomenon, one can try to use the effective medium model [16]. In spite of the fact that particle sizes in our case are greater than the wavelength of light and applicability of this model is not quite justified, main properties of the medium are probably also described (at least qualitatively) in this model. Let us use the Maxwell-Garnett model. Dielectric permittivity of the effective medium ε_{eff} consisting of several components can be found as a solution of the equation:

$$\sum_{i=1}^{N} f_i \theta_i (\varepsilon_{eff} - \varepsilon_i) = 0. \quad (1)$$

Here, ε_i are dielectric permittivities of the medium components, f_i is the filling factor of the component i, and θ_i is the formfactor of the component i. In addition, the normalization condition:

$$\sum_{i=1}^{N} f_i = 1\,,\ \sum_{i=1}^{N} \theta_i = 1 \qquad (2)$$

must be satisfied. The sample anisotropy can be related both to the shape anisotropy and to the anisotropic distribution of microcrystals. In the case of random orientation of microcrystals, the sample anisotropy can be related only to the dependence of the filling factor on the direction.

From the obtained data we can estimate anisotropy of the filling factor. The average thickness of the sample is estimated by the quantity of deposited material and amounts to about 5 μm. The presence of the optical axis results in the fact that the ordinary and extraordinary rays propagate with different phase velocities. This manifests itself in conversion of linear polarization to circular polarization. If the sample thickness is such that the phase difference of these rays is multiple 2π, polarization conversion does not occur. This is just the isotropic point in the spectrum. From this it follows that the difference of the effective refractive indices $\sqrt{\varepsilon_{eff}^{\parallel}} - \sqrt{\varepsilon_{eff}^{\perp}} \approx 0.15$ and, therefore, anisotropy of the filling factor $f^{\parallel} - f^{\perp}$is only 0.08. Such small value cannot be strongly pronounced but is observed in transmission spectra.

We believe that, in our case, microcrystals obtained by splitting of bulk BN crystals in an ultrasonic bath are electrized due to bond opening and then, in the process of deposition, they agglomerate in an orderly fashion according to the direction of the dipole moment. As a result of such anisotropic correlations in the distribution of microcrystals, their density can turn out to be different in different directions. It can be not seen by sight (see Fig. 1a in [13]) but can manifest itself in polarization. Indeed, the electrostatic fields can turn out to be sufficient for ordering of dielectric crystals in the process of their electrification.

4. Conclusions

Thin hexagonal boron nitride films with a thickness of several monoatomic layers have been manufactured by cleavage of bulk samples in an ultrasonic bath. The transmission, reflection, and photoluminescence spectra of such films have been studied in the region below the fundamental absorption edge. The spectral dependences of linear and circular polarization of light passing through the sample have been measured. The examination with the use of scanning electron microscopy demonstrates the absence of visible preferred directions in the sample. However, the consideration of Stokes parameters of light passing through the sample revealed the phenomenon of birefringence. It has been found that the optical axes have the same direction over the whole area of the sample. At the same time, the light scattered by the sample is not polarized. This points to the fact that the anisotropy is caused not by properties of individual microcrystals but is common for the whole sample and is related to anisotropy of the filling factor.

Conflict of interest

The authors declare that they have no conflicts of interest.

References

1. P. Moon and M. Koshino, Phys. Rev. B **90**, 155406 (2014).
2. C. Ronning, A. D. Banks, B. L. McCarson, R. Schlesser, Z. Sitar, R. F. Davis, B. L. Ward, and R. J. Nemanich, J. Appl. Phys. **84**, 5046 (1998).
3. B. T. Hogan, E. Kovalska, M. O. Zhukova, M. Yildi- rim, A. Baranov, M. F. Craciun, and A. Baldycheva, Nanoscale **11**, 16886 (2019).
4. A. Akbari, P. Sheath, S. T. Martin, D. B. Shinde, M. Shaibani, P. C. Banerjee, R. Tkacz, D. Bhattacha- ryya, and M. Majumder, Nat. Commun. **7**, 10891 (2016).
5. K. Fu, Y. Wang, C. Yan, Y. Yao, Y. Chen, J. Dai, S. Lacey, Y. Wang, J. Wan, T. Li, Z. Wang, Y. Xu, and L. Hu, Adv. Mater. **28**, 2587 (2016).
6. R. Jalili, S. Aminorroaya-Yamini, T. M. Benedetti, S. H. Aboutalebi, Y. Chao, G. G. Wallace, and D. L. Officer, Nanoscale **8**, 16862 (2016).
7. P. Shaban, E. Oparin, M. Zhukova, B. Hogan, E. Ko- valska, A. Baldycheva, and A. Tsypkin, AIP Conf. Proc. **2300**, 020111 (2020).
8. B. T. Hogan, E. Kovalska, M. F. Craciun, and A. Baldycheva, J. Mater. Chem. C **5**, 11185 (2017).
9. D.-W. Shin, M. D. Barnes, K. Walsh, D. Dimov, P. Tian, A. I. S. Neves, C. D. Wright, S. M. Yu, J.-B. Yoo, S. Russo, and M.

F. Craciun, Adv. Mater. **30**, 1802953 (2018).
10. M. O. Zhukova, B. T. Hogan, E. N. Oparin, P. S. Shaban, Y. V. Grachev, E. Kovalska, K. K. Walsh, M. F. Cra- ciun, A. Baldycheva, and A. N. Tcypkin, Nanoscale Res. Lett. **14**, 225 (2019).
11. S. N. Grinyaev, F. V. Konusov, and V. V. Lopatin, Phys. Solid State **44**, 286 (2002).
12. T. B. Ngwenya, A. M. Ukpong, and N. Chetty, Phys. Rev. B **84**, 245425 (2011).
13. G. Jacucci, J. Bertolotti, and S. Vignolini, Adv. Opt. Mater. **7**, 1900980 (2019).
14. A. Segure, L. Artus, R. Cusco, T. Taniguchi, G. Cassabois, and B. Gil, Phys. Rev. Mater. **2**, 024001 (2018). 15. L. V. Kotova, A. V. Platonov, A. V. Roshakinsky, and T. V. Shubina, Semiconductors **54**, 1509 (2020).
16. A. P. Vinogradov, in *Electrodynamics of Composite Materials*, Ed. by B. Z. Katsenelenbaum (Editorial URSS, Moscow, 2001), p. 208 [in Russian]